Optical breakdown thresholds for transparent microparticles irradiated with laser pulse of the nano-, pico-, and femtosecond duration

A.A. Zemlyanov and Yu.E. Geints

Institute of Atmospheric Optics,
Siberian Branch of the Russian Academy of Sciences, Tomsk

We consider the initial stage of the plasma formation due to optical breakdown near aerosol particles in the field of an intense laser radiation. The intensity threshold of the optical breakdown of transparent microparticles exposed to radiation of a single laser pulses of nano-, pico-, and femtosecond duration is calculated based on the nonstationary Mie theory and numerical solution of the rate equation for the electron concentration in plasma. It is shown that the femtosecond mode of optical breakdown of a particle is characterized by a higher (approximately by two orders of magnitude) initiation threshold as compared with the breakdown under the exposure to nano- and picosecond-duration pulses, as well as by higher concentration of free electrons near the external focal point for the radiation incident on the particle.

Introduction

The interaction of an intense laser radiation of nanosecond and picosecond duration with aerosol is accompanied by the effect of optical breakdown near aerosol particles.[1] It has been found that in the case of absorbing particles the breakdown initially occurs in the dense vapor produced by evaporation of the particle exposed to the radiation. For weakly absorbing particles, the plasma of the optical breakdown is first produced inside the particle, and then the optical discharge propagates outside into the gas medium. Some experiments on the optical breakdown of transparent condensed media (quartz, sapphire, glass, water) under the effect of femtosecond laser pulses are known.[2,3] The appearance of optical breakdown was observed as the glowing plasma filament in the substance and the intense acoustic signal from the region of the light beam.

In atmospheric optics, the optical breakdown of aerosol microparticles is discussed, first of all, as a source of plasma for emission analysis of the particulate matter[1] and as a source for creation of an ionized channel and formation of extended filaments at propagation of high-power femtosecond pulses in clouds.[4] The thresholds and dynamics of the development of the optical breakdown in particles are also important for evaluation of the possibility of mechanically destructing the microparticle due to dissipation of the energy stored in plasma and, in addition, in the problems of laser energy transport through the atmosphere by a series of femtosecond pulses.[5]

The objective of this paper is theoretical calculation of the optical breakdown thresholds for transparent microparticles exposed to single laser pulses with the nano-, pico-, and femtosecond duration.

Rate equation for the electron concentration in plasma

The formation of plasma in the medium upon propagation of an intense laser radiation is connected with the generation of free electrons under the effect of light field. The main physical mechanisms of photoionization of the condensed and gaseous media are the cascade (avalanche) and multiphoton ionization (MPI). The particular role of each of these ionization mechanisms in plasma formation depends on the intensity and duration of the laser pulses.

The evolution of the electron concentration in plasma is considered theoretically based on the system of kinetic (rate) equations for the concentrations of negatively n_e and positively n_p charged and neutral particles, which account for all the physical mechanisms regulating the charge balance in plasma (see, for example, Refs. 6 and 7). However, under conditions of quasineutral ($n_p \approx n_e$) and quasiequilibrium plasma (we are speaking about the thermodynamic equilibrium), only one rate equation for n_e turns out sufficient in the most cases:

$$\frac{\partial n_e}{\partial t} = \eta_{mpa} I^m + \eta_{cas} I n_e - \eta_{rec} n_e^2 - \eta_{att} n_e . \qquad (1)$$

Here η_{mpa}, η_{cas}, η_{rec}, η_{att} are the parameters characterizing the rates of MPI, cascade ionization, recombination, and attachment of electrons, respectively; I is the intensity of laser radiation; m is the integer part of the sum $(E_i/\hbar\omega_0 + 1)$; E_i is the energy of atom ionization; ω_0 is the central frequency in the laser pulse spectrum; $\hbar$ is the Planck constant.

The first two terms in the right-hand side of Eq. (1) describe the growth of the concentration of free electrons, while the others characterize its decrease.

At the cascade ionization, the seed free electrons, which are always present in the medium, gain the energy in the electromagnetic field of the beam due to the effect of backward deceleration emission and can ionize neutral atoms colliding with them. The new generated electrons, interacting with the light field, also increase their energy and cause formation of a new portion of free charges, and so on. Thus, an electron avalanche develops in the medium, and the concentration of free electrons n_e in it grows exponentially with time.[8,9]

The rate of cascade ionization in the approximation of instantaneous energy exchange between the electron and the atom (Drude model) is expressed as follows[8]:

$$\eta_{cas} = \frac{1}{(\omega_0\tau_{coll})^2 + 1}\frac{\tau_{coll}\mathbf{e}^2}{n_a c\varepsilon_0 m_e E_i}, \qquad (2)$$

where m_e and $\mathbf{e}$ are the electron mass and charge; ε_0 is the electric constant; n_a is the refractive index of the medium; τ_{coll} is the electron mean free time, the time between collisions.

According to MPI theory developed by L.V. Keldysh,[10] an atom can be also ionized as a result of successive absorption of several radiation quanta. In this case, the bound electron receives the energy sufficient to leave the atom and form the gas of free electrons. The probability of this process is proportional to the instantaneous intensity of laser radiation to the mth power. Unlike the cascade ionization, MPI requires rather high radiation intensity, but evolves much faster.

For calculation of the MPI rate, the equations from Ref. 10 can be used:

$$\eta_{mpa} = \frac{2\omega_0}{9\pi}\left(\frac{m'_e\omega_0}{\hbar}\right)^{3/2}\left(\frac{\mathbf{e}^2}{16 n_a c\varepsilon_0 m'_e\omega_0^2 E_i}\right)^m \exp(2m)\Phi(\xi),$$
$$(3a)$$

$$\eta_{mpa} = N_0\omega_0\left(\frac{E_i}{\hbar\omega_0}\right)^{3/2}\left(\frac{\mathbf{e}^2}{4 n_a c\varepsilon_0 m_e\omega_0^2 E_i}\right)^m, \qquad (3b)$$

where $m'_e \approx m_e/2$ is the reduced exciton mass; N_0 is the concentration of neutral gas molecules;

$$\xi = \sqrt{2(m - E_i/\hbar\omega_0)}; \ \ \Phi(\xi) = \exp(-\xi^2)\int_0^\xi \exp(\zeta^2)d\zeta$$

is the Dawson's integral. Equation (3a) is used for condensed media, and Eq. (3b) is for the gaseous ones.

Note that at an extremely high intensity of radiation acting on the medium $I \sim 10^{13}-10^{15}$ W/cm^2, one more photoionization mechanism is possible, namely, tunnel ionization.[11] In this case, the electron in atom is capable of tunneling through the ionization potential barrier, absorbing much less light quanta than in the case of MPI. Thus, for example, according to the data of the experimental paper,[12] about seven light quanta ($m = 7$) are needed for tunnel ionization of nitrogen (N_2) atoms by a femtosecond-duration radiation pulse of a Ti:sapphire laser with the central wavelength $\lambda_0 = 800$ nm, while MPI requires $m = 11$. For oxygen (O_2) these parameters are respectively 6 and 9. However, in this paper, we do not consider this mechanism of ionization, and, thus, the threshold of optical breakdown given below should be considered as the upper limit for the intensity of incident laser radiation.

The physical processes leading to the decrease of the electron concentration in plasma are the electron–ion recombination and the capture of free electrons by neutral molecules of the medium with formation of negative ions, i.e., the so-called attachments of electrons.[8] The rate of electron recombination, which, in essence, is the process inverse to ionization, is proportional to the concentration of positive ions n_p and the frequency of collisions of electrons and ions in plasma ν_{coll}. The typical values of the last parameter in the plasma with the subcritical electron concentration are $\nu_{coll} \approx 10^{13}$ s^{-1} for the atmospheric air[8] and $\nu_{coll} \approx 10^{15}$ s^{-1} in water.[13] The characteristic time of electron attachment was estimated as $\tau_{att} \sim 4{\cdot}10^{-8}$ s for oxygen[14] and $\tau_{att} \sim 10^{-11}$ s for water.[13]

For the rate of the electron–ion recombination there are the following experimental estimates: $\eta_{rec} \approx 1.1\cdot10^{-12}$ m^3/s for the atmospheric air[14] and $\eta_{rec} \approx 2.0\cdot10^{-15}$ m^3/s for water.[13,15] The process of capture of free electrons by neutral molecules and formation of negative ions is described by the corresponding rate of attachment[8]:

$$\eta_{att} = \frac{m_e\tau_{coll}\omega_0^2}{M\left[(\omega_0\tau_{coll})^2 + 1\right]}, \qquad (4)$$

where M is the mass of molecule.

The basic regularities of the development of the electron avalanche in the medium under the effect of laser radiation can be followed through solution of Eq. (1) for the model pulse with the rectangular time shape of the intensity

$$I(t) = I_0\left[\Theta(t) - \Theta(t_p)\right],$$

where $\Theta(t)$ is the unit stepwise Heaviside function; t_p is the laser pulse duration. The solution of Eq. (1) obtained by the Bernoulli method looks as follows:

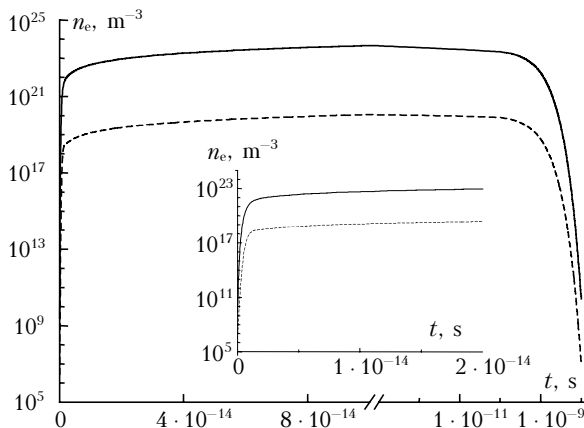$$n_e(t) = n_{e0} + \frac{\mu}{2\eta_{rec}}\tanh h\left(\frac{\mu}{2}t\right), \ \ t \le t_p,$$

$$n_e(t) = \frac{\eta_{att}}{\eta_{rec} + \exp[\eta_{att}(t - t_p)](\eta_{att}/n_e(t_p) + \eta_{rec})}, \ t > t_p.$$

Here n_{e0} is the initial concentration of free electrons in the medium;

$$\mu = \sqrt{(\eta_{cas}I_0 - \eta_{att})^2 + \eta_{rec}\eta_{mpa}I^m} \ .$$

The evolution of the concentration n_e is shown in Fig. 1. The parameters of calculation were the following:

the radiation pulse: $\lambda_0 = 800$ nm; $I_0 = 10^{11}$ W/cm²; $t_p = 10^{-13}$ s;

medium: water, $n_{e0} = 1$ m⁻³; $m = 5$; $E_i = 6.5$ eV; $\eta_{mpa} = 2.51 \cdot 10^{-48}$ m⁷·s⁴/J⁵; $\eta_{cas} = 1.93 \cdot 10^{-4}$ m²/J.

Fig. 1. Evolution of the concentration of free electrons in water under the exposure to a rectangular-shaped radiation pulse with the account of MPI and cascade ionization (solid curve) and at $\eta_{cas} = 0$ (dashed curve). The inserted fragment demonstrates the initial stage of the development of the electron avalanche.

It can be seen that after the quick growth the concentration of plasma electrons achieves the level of saturation, which, as will be shown below, depends on the intensity of the incident light wave. At $t > t_p$ (the time $t = t_p$ corresponds to the break of abscissa on the plot), n_e begins to decrease first as $1/t$ due to the mechanism of electron–ion recombination and then exponentially for the time $t \approx \eta_{att}^{-1}$ due to the attachment of electrons to neutral atoms. The maximum achievable level of the concentration of free electrons follows from Eq. (5) under the condition that $\mu \gg 1$:

$$n_{e\,max} = n_{e0} + \frac{\mu}{2\eta_{rec}},$$

and within the framework of the model used it is proportional to the radiation intensity $I_0^{m/2}$.

To determine the fractions of MPI and cascade ionization in evolution of the plasma, $n_e(t)$ was calculated by Eq. (5) at $\eta_{cas} = 0$. The results of this calculation are shown by the dashed curve in Fig. 1. The level of $n_{e\,max}$ turned out to be much lower in this case. This indicates that in the condensed medium (water) the role of MPI reduces to provision of seed electrons for the following development of the avalanche just due to cascade ionization.

At the same time, MPI, as known,[11] plays a certain role in plasma formation in the gas medium at high intensity of the laser radiation. This is also confirmed by our calculations for the atmospheric air (78% N_2 and 22% O_2) at the following parameters:

$$E_i(N_2) = 15.6 \text{ eV } (m = 11),$$
$$E_i(O_2) = 12.5 \text{ eV } (m = 9);$$
$$\eta_{mpa}(N_2) = 5.75 \cdot 10^{-165} \text{ m}^{19} \cdot \text{s}^{10}/\text{J}^{11},$$
$$\eta_{mpa}(O_2) = 8.21 \cdot 10^{-127} \text{ m}^{15} \cdot \text{s}^8/\text{J}^9;$$
$$\eta_{cas} = 8.32 \cdot 10^{-7} \text{ m}^2/\text{J},$$
$$\eta_{rec} = 1.1 \cdot 10^{-13} \text{ m}^3/\text{s}, \ \eta_{att} = 2.5 \cdot 10^7 \text{ s}^{-1}.$$

In this case, to obtain the concentration of free electrons $n_{e\,max} \sim 10^{24}$ m⁻³, the radiation intensity has been increased up to $I_0 = 10^{14}$ W/cm².

Discussion

Consider the results of numerical simulation of the optical breakdown in the vicinity of water droplets suspended in air. The electron concentration in plasma was calculated by Eq. (1) with the account of Eqs. (2)–(4) based on the 4th-order Runge–Kutta numerical scheme. First, the model problem on the nonstationary scattering of a plane light wave at a spherical particle was solved by the method described in Ref. 16. This yielded the dependence of the relative intensity of the optical field (inhomogeneity factor $B(\mathbf{r}; t) = I(\mathbf{r}; t)/I_0$) at some spatial points corresponding to the radiation intensity maxima in the illuminated (point 1 in Fig. 2) and the shadow (point 2) hemispheres of the droplet and in the region of the geometrical focus beyond the particle near its rear surface (point 3). Then the function $B(\mathbf{r}; t)$ was used in solution of Eq. (1).
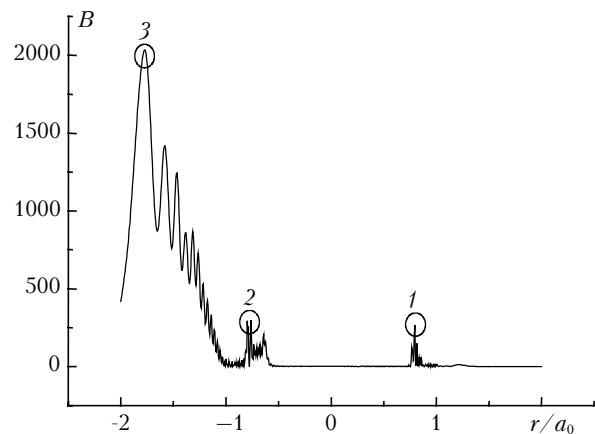
Fig. 2. Distribution of the factor B along the principal diameter of the water droplet (radius $a_0 = 50$ μm; $n_a = 1.33$) exposed to the plane monochromatic wave with $\lambda_0 = 800$ nm. Circles mark the intensity maxima of the optical field in the illuminated (1) and shadow (2) hemispheres and the region of geometric focus (3). The radiation is incident from the right to the left.

This choice of the spatial points for the calculation of $n_e(t)$ was caused by the highest

probability of formation of the plasma of the primary optical breakdown just at the places of intensity maxima of the optical field.

The time dependences of the relative intensity at the points *1–3* upon scattering of the 50-fs pulse ($\lambda_0 = 800$ nm) with the Gaussian time profile

$$I(t) = I_0 \exp\{-[(t - t_0)/t_p]^2\},$$

where t_p is the pulse duration, t_0 is a parameter, are shown in Fig. 3. The zero time here corresponds to the time, when the leading edge of the pulse reaches the illuminated hemisphere of the droplet.
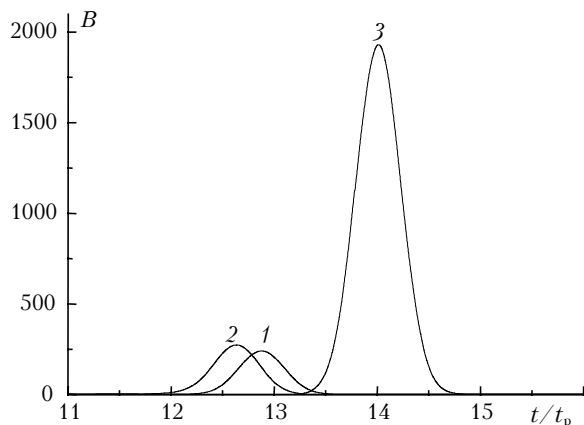
Fig. 3. Time dependence of the relative intensity of the optical field at the points of the front (*1*), rear (*2*), and external (*3*) maxima at the incidence of the radiation pulse $t_p = 50$ fs, $t_0 = 100$ fs on a water droplet ($a_0 = 50$ μm; $n_a = 1.33$).

It follows from Fig. 3 that at the nonstationary scattering of radiation in the particle, the dependence $B(t)$ at the chosen points almost exactly copies the profile of the initial radiation pulse, is shifted in time due to the pulse propagation through the particle.[17] First, the maximum of the internal optical field is formed in the shadow hemisphere of the particle (point *2*); then, as the light wave is reflected from the rear surface of the droplet, the intensity maximum is formed in the illuminated hemisphere (point *1*). Finally, the external intensity maximum is formed (point *3*) near the rear surface of the particle. The maximum intensity of the optical field achievable for the exposure time (B_m) in the particle of the given size turned out practically identical at the points of the front and rear maxima: $B_m = 239.8$ (point *1*) and $B_m = 272.5$ (point *2*). At the same time, B_m at the point of the external field focus is almost sevenfold as high as these values: $B_m = 1930.5$ (point *3*).

The evolution of the concentration of the plasma electrons at the chosen points is shown in Fig. 4. The concentration values are normalized to $n_e^{th} = 10^{26}$ m^{-3}, which are close to the experimentally measured threshold, whose excess initiates the optical breakdown in the medium.[13]
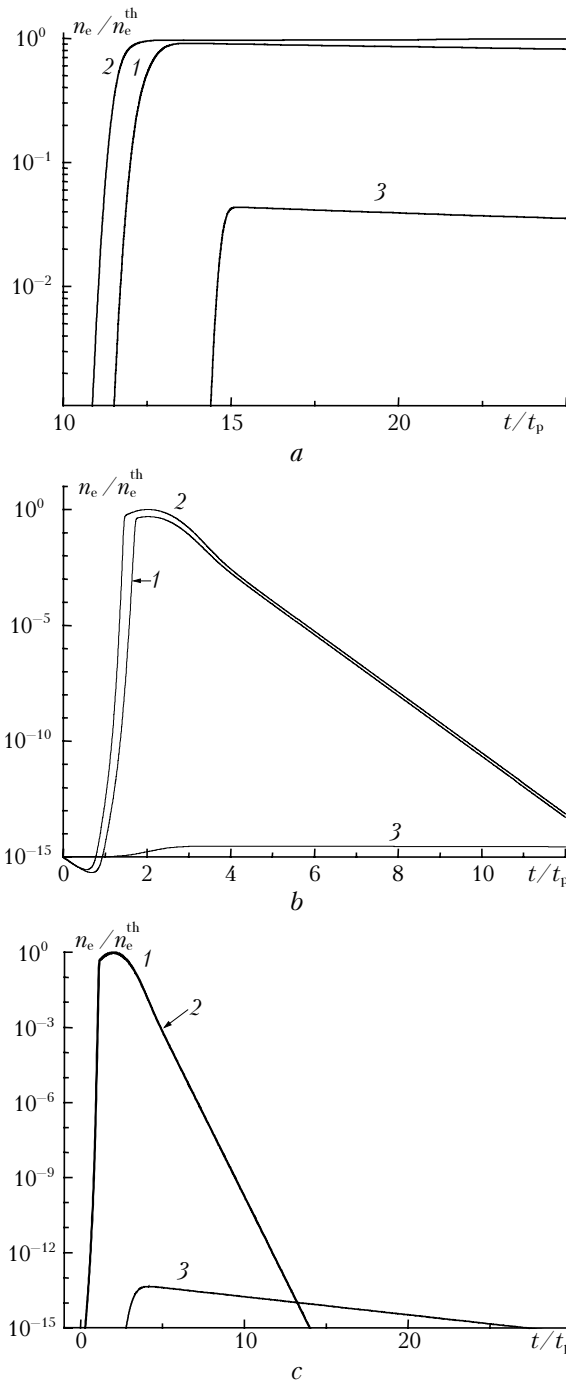
Fig. 4. Time dependence of the relative electron concentration in plasma n_e/n_e^{th} at the points of the front (*1*), rear (*2*), and external (*3*) maxima at incidence of the pulse with $\lambda_0 = 800$ nm on the water droplet ($a_0 = 50$ μm; $n_a = 1.33$): $t_p = 50$ fs, $t_0 = 100$ fs, $I_0 = 1.18 \cdot 10^{11}$ W/cm^2 (*a*); $t_p = 1$ ps, $t_0 = 2$ ps, $I_0 = 1.1 \cdot 10^9$ W/cm^2 (*b*); $t_p = 1$ ns, $t_0 = 2$ ns, $I_0 = 7.9 \cdot 10^8$ W/cm^2 (*c*). Curves *1* and *2* coincide.

The intensity of the incident radiation corresponding to this threshold for the droplet of the radius $a_0 = 50$ μm was $I_0^{th} = 1.18 \cdot 10^{11}$ W/cm^2, which is two orders of magnitude higher than the threshold intensity of the breakdown of water droplets in air

for nanosecond pulses of the second harmonic of a Nd:YAG laser ($\lambda_0 = 532$ nm) $I_0^{th} = 2.5 \cdot 10^9$ W/cm^2 [Ref. 18] and, at the same time, two orders of magnitude lower than the breakdown threshold for clean air (without aerosol) $I_0^{th} = 4-6 \cdot 10^{13}$ W/cm^2 ($\lambda_0 = 800$ nm) [Ref. 12]. At the same time, the radiation energy density needed for initiation of the optical breakdown in the particle exposed to the pulse with $t_p = 50$ fs is only $w^{th} \sim 2$ mJ/cm^2, while the same parameter in water for the picosecond pulse is $w^{th} \sim 400-650$ mJ/cm^2 [Ref. 19].

As can be seen from Fig. 4, the threshold intensity of free electrons is achieved at the chosen irradiation intensity only at the rear focus. In the illuminated hemisphere, the values of n_e are also close to, but still lower than n_e^{th}. In this case, the maximum electron concentration n_e is only $\sim 0.05\, n_e^{th}$ in the zone of the geometric focus of the incident radiation ($r/a_0 = -1.77$), in spite of the significantly higher intensity of the optical field and, consequently, the probability of breakdown here is lower.

For a comparison, Fig. 4 shows the dependence $n_e(t)$ at the incidence of the picosecond and nanosecond pulses onto the water droplet. The intensity of the incident radiation in this case was much lower: $I_0 = 1.1 \cdot 10^9$ and $7.9 \cdot 10^8$ W/cm^2, respectively. It should be noted that here the concentration of free electrons in the internal zones of the droplet by the time of optical breakdown is already more than 12 orders of magnitude higher than outside the particle due to, first of all, the higher rate of cascade ionization of water as compared to that of atmospheric gases.

Using the solution (4) for a model rectangular-shaped pulse, we obtain the equation for the threshold of the optical breakdown of the medium in the presence of the aerosol particle under the condition $n_e(I_0^{th}) = n_e^{th}$. For short pulses, when the ionization of the medium is determined predominantly by the MPI mechanism, the replacement of the hyperbolic tangent function by its asymptotic at small argument values gives

$$I_0^{th} \approx \left[\frac{n_e^{th}}{t_p \eta_{mpa} B_m} \right]^{1/m}. \tag{5}$$

In the mode of long pulses, when the process is largely determined by the cascade ionization of the medium, the corresponding estimate of the threshold breakdown intensity has the form

$$I_0^{th} \approx \frac{1}{\eta_{cas} B_m} \left[2\eta_{rec} n_e^{th} + \eta_{att} \right] \tag{6}$$

and is independent of the laser pulse duration. In these equations, the role of the particle is taken into account by the factor B_m showing the degree of the

growth of the optical field intensity over the intensity of the incident radiation as a result of its internal and external focusing by the particle surface.

Note that this dependence of the breakdown threshold on the laser pulse duration was discussed earlier in the theoretical paper[20] for a bulk water medium based on the numerical calculation by Eq. (1). Here we would like only to emphasize that though the presence of a microparticle decreases the threshold of the optical breakdown both inside and outside the particle, for the femtosecond radiation this effect is less pronounced than for the nano- and picosecond pulses.

Conclusions

Thus, the results presented indicate that the physical pattern of appearance of the optical breakdown of weakly absorbing microparticles is the same for both long and ultrashort pulses. The plasma is first formed at the rear focus inside the particle, and then, if the exposure to the radiation continues, the optical breakdown is possible in the gas medium adjacent to the particle in the region of the geometric focus of the particle for the incident radiation. The main difference of the femtosecond mode of optical breakdown from the breakdown under the exposure to pico- and nanosecond laser pulses is in the higher ($\sim 10^2$ times) threshold intensities of the incident radiation, as well as in a more significant role of the external focal zone of the optical field diffracted at the particle in the process of formation of the primary plasma.

Acknowledgments

References

1. V.E. Zuev, A.A. Zemlyanov, Yu.D. Kopytin, and A.V. Kuzikovskii, *High-Power Laser Radiation in Atmospheric Aerosols* (D. Reidel Publ. Corp., Holland, Dordrecht, 1984), 291 pp.
2. D. Linde and H. Schuler, J. Opt. Soc. Am. B **13**, No. 1, 213−222 (1996).
3. E. Abraham, K. Minoshima, and H. Matsumoto, Opt. Commun. **176**, 441−452 (2000).
4. F. Courvoisier, V. Boutou, J. Kasparian, E. Salmon, G. Méjean, J. Yu, and J.-P. Wolf, Appl. Phys. Lett. **83**, No. 2, 213−215 (2003).
5. A. Couairon, G. Méchain, S. Tzortzakis, M. Franco, B. Lamouroux, B. Prade, and A. Mysyrowicz, Opt. Commun. **225**, 177−192 (2003).
6. X.M. Zhao, J.-D. Diels, C.Y. Wang, and J.M. Elizondo, IEEE J. Quant. Electron. **31**, 599−612 (1995).
7. S. Tzortzakis, B. Prade, M. Franco, and A. Mysyrowicz, Opt. Commun. **181**, 123−127 (2000).
8. Yu.P. Raizer, *Physics of Gas Discharge* (Nauka, Moscow, 1987), 592 pp.

9. E. Yablonovitch and N. Bloembergen, Phys. Rev. Lett. **29**, No. 9, 581–584 (1972).

10. L.V. Keldysh, Zh. Eksp. Teor. Fiz. **47**, 1945–1956 (1964).

11. N.B. Delone and V.P. Krainov, *Nonlinear Ionization of Atoms by Laser Radiation* (Fizmatlit, Moscow, 2001), 311 pp.

12. A. Talebpour, J. Yang, and S.L. Chin, Opt. Commun. **163**, 29–32 (1999).

13. C.H. Fan, J. Sun, and J.P. Longtin, J. Appl. Phys. **91**, No. 4, 2530–2536 (2002).

14. J. Schwarz and J.-C. Diels, Phys. Rev. A **65**, 013806-1– 013806-10 (2001).

15. F. Docchio, Europhys. Lett. **6**, 407–412 (1988).

16. A.A. Zemlyanov and Yu.E. Geints, Atmos. Oceanic Opt. **15**, No. 8, 619–627 (2002).

17. A.A. Zemlyanov and Yu.E. Geints, Atmos. Oceanic Opt. **16**, No. 10, 822–825 (2003).

18. P. Chýlek,   M.A. Jarzembski,   V. Srivastava, R.G. Pinnick, J.D. Pendleton, and J.P. Cruncleton, Appl. Opt. **26**, No. 5, 760–762 (1987).

19. A. Vogel, J. Noack, K. Nahen, D. Theisen, S. Busch, U. Parlitz, D.X. Hammer, G.D. Noojin, B.A. Rockwell, and R. Birngruber, Appl. Phys. B **68**, 271–280 (1999).

20. J. Noack and A. Vogel, IEEE J. Quant. Electron. **35**, No. 8, 1156–1167 (1999).